The Innovation

Report

Highly efficient conversion of surplus electricity to hydrogen energy via polysulfides redox

Mo Zhang,[1,2,4] Jing Guan,[3,4] Yunchuan Tu,[1,2] Suheng Wang,[1,2] and Dehui Deng[1,2,*]
*Correspondence: dhdeng@dicp.ac.cn
Received: March 25, 2021; Accepted: July 12, 2021; Published Online: July 15, 2021; https://doi.org/10.1016/j.xinn.2021.100144

Graphical abstract

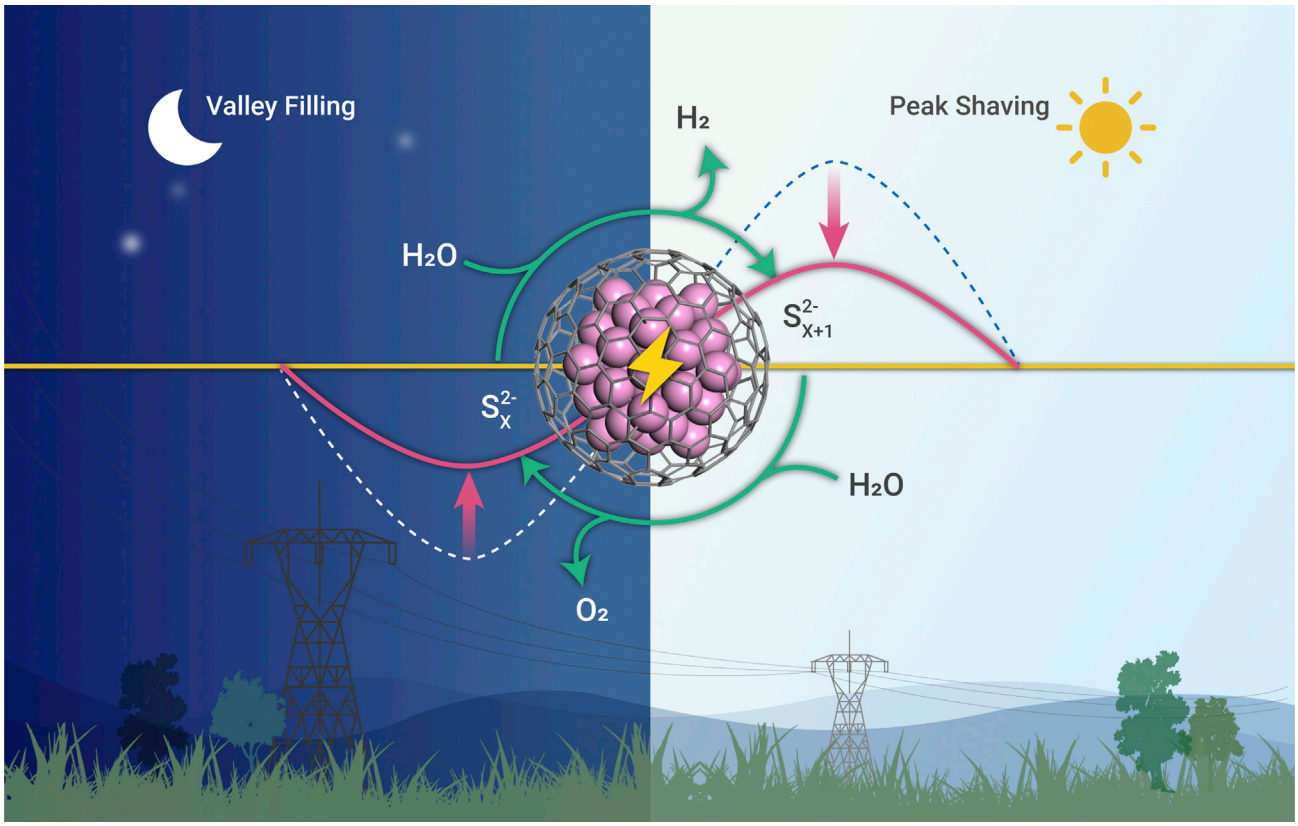

Public summary

- A high-performance device of decoupled water electrolysis is constructed by using polysulfides as mediators and graphene-encapsulated CoNi as catalysts, which provides a new strategy to distribute the electricity reasonably by peak shaving and valley filling
- The potential of H_2 production only needs 0.82 V at 100 mA/cm^2 current density, which saves 60.2% more energy than direct electrolysis of water
- The capacity of the electrolyzer to produce voluminous hydrogen reaches 2.5 × 10^5 mAh/cm^2 in a single pass, which is the highest capacity reported so far
- The device exhibits superior cyclicity in 15-days periodic recycle tests without any decay of performance

Highly efficient conversion of surplus electricity to hydrogen energy via polysulfides redox

Mo Zhang,[1,2,4] Jing Guan,[3,4] Yunchuan Tu,[1,2] Suheng Wang,[1,2] and Dehui Deng[1,2,*]

[1]State Key Laboratory of Physical Chemistry of Solid Surfaces, Collaborative Innovation Center of Chemistry for Energy Materials (iChEM), College of Chemistry and Chemical Engineering, Xiamen University, Xiamen 361005, China

[2]State Key Laboratory of Catalysis, iChEM, Dalian Institute of Chemical Physics, Chinese Academy of Science, Zhongshan Road 457, Dalian 116023, China

[3]School of Environmental & Municipal Engineering, Qingdao University of Technology, Qingdao 266033, China

[4]These authors have contributed equally

*Correspondence: dhdeng@dicp.ac.cn

Received: March 25, 2021; Accepted: July 12, 2021; Published Online: July 15, 2021; https://doi.org/10.1016/j.xinn.2021.100144

Citation: Zhang M., Guan J., Tu Y., et al., (2021). Highly efficient conversion of surplus electricity to hydrogen energy via polysulfides redox. The Innovation **2(3)**, 100144.

Decoupled electrolysis of water is a promising strategy for peak load regulation of electricity. The key to developing this technology is to construct decoupled devices containing stable redox mediators and corresponding efficient catalysts, which remains a considerable challenge. Herein, we designed a high-performance device, using polysulfides as mediators and graphene-encapsulated CoNi as catalysts. It produced H_2 with a low potential of 0.82 V at 100 mA/cm^2, saving 60.2% more energy than direct water electrolysis. The capacity of H_2 production reached 2.5×10^5 mAh/cm^2, which is the highest capacity reported so far. This device exhibited excellent cyclability in 15-day recycle tests, without any decay of performance. The calculation results revealed that the electronic structure of the graphene shell was modulated by the electron transfer from N-dopant and metal core, which significantly facilitated recycle of polysulfides on graphene surfaces. This study provides a promising method for constructing a smart grid by developing efficient decoupled devices.

Keywords: peak shaving and valley filling; decoupled electrolysis; H_2 production; chainmail catalyst; polysulfides redox

INTRODUCTION

The imbalance between the generation and consumption of electricity raises challenges in the efficient utilization of electricity. As related to human life and production, the electricity consumption exists peaks in the daytime and valleys at night. With a constant generation mode of electricity that meets the demand in the peak time, there are huge amounts of surplus electricity during the valley time. Therefore, it is important to find an efficient method of storing surplus electricity and releasing it when demanded, which realizes the efficient utilization of electricity by peak shaving and valley filling.[1,2]

H_2 is advocated as a green energy carrier, so producing H_2 from water electrolysis is a promising strategy for the conversion of surplus electricity to sustainable clean energy.[3–5] As the conventional electrolysis of water contains the disadvantage of gas crossover (H_2 and O_2) and problems in H_2 storage and transportation, the decoupled electrolysis is proposed against this backdrop.[6,7] Through the utilization of redox mediators, the electrolysis of water could be decoupled into two steps. Step1 is O_2 evolution reaction (OER) with the reduction of the mediator, and step 2 is H_2 evolution reaction (HER) with the oxidation of the mediator.[7,8] As the anode potential for the oxidation of the mediator is lower than the OER, the energy cost is reduced in the step of H_2 production. Therefore, the decoupled water electrolysis is helpful to produce H_2 with high purity and low price. By introducing decoupled devices into the peak regulation system, a kind of strategy can be designed to convert surplus electricity to hydrogen energy, achieving the peak shaving and valley filling. The specific method is that proceeding step 1 in the valley time, which stores the cheap and unused surplus electricity in the reduced mediator for valley filling (step 1). Then the oxidation of the mediator in step 2 would produce H_2 with low energy consumption. In the peak time, the produced H_2 could connect to the users directly and reduce the cost of H_2 storage. The development of such technology relies on an appropriate redox mediator and corresponding catalyst of the decoupled electrolyzer. However, it is still greatly limited by the small capacity of the electrolyzer and the low activity of electrode for H_2 production.[7,9–11] Therefore, it is urgent to develop a high-performance decoupled device with a high-capacity electrolyzer and high-activity electrode.

S is a cheap chemical that has abundant reserves on the Earth.[12] Its redox polysulfides (S_{x+1}^{2-}/S_x^{2-}), which have a simple structure and high solubility in alkaline solutions, could maintain great cyclability of redox by the catalysis of the appropriate electrode. In the previous work, the N-doped graphene encapsulating CoNi nanoalloy material (CoNi@NGs) could resist the corrosion of sulfide and presented excellent performance in the sulfide oxidation reaction.[13] Inspired by this, we herein introduced polysulfides into the decoupled electrolyzer as the redox mediator, and ingeniously employed CoNi@NGs to prepare redox electrodes. It successfully decoupled the process of water electrolysis into separate HER and OER steps. With the efficient catalysis of CoNi@NGs, this device could produce significant amounts of H_2 with low energy consumption and exhibited excellent cyclability in the extensive recycle tests. This resulting electrolyzer achieved the highly efficient conversion of surplus electricity to hydrogen energy.

RESULTS

Mechanism of decoupled water electrolysis

The operation mechanism of decoupled electrolyzer is shown in Figure 1A, which includes two steps. Step 1 (valley time, usually at night) involved a cathodic polysulfides reduction reaction (SRR) and anodic OH^- oxidation for OER (O_2 production). In the subsequent step 2 (peak time, usually in the daytime), the reduction of H_2O for HER (H_2 production) occurred on the cathode and the polysulfides oxidation reaction (SOR) happened simultaneously on the anode. Both electrodes were coated with the CoNi@NGs catalyst, which was prepared through a template-assisted method. Its synthesis method is detailed in the supplemental information. As the transmission electron microscopy (TEM) images shown in Figures 1B and S1, the CoNi@NGs consisted of CoNi nanoparticles completely encapsulated by a single-layer graphene shell distributed on the interlaced carbon nanotubes. The lattice fringes of the internal metal displayed an interplanar spacing of 2.1 Å, which matched well with the (111) plane of the CoNi alloy. The graphene shells protect the CoNi metal cores from corrosion in the harsh reaction environment.[13]

Before fabricating the electrolyzer, the electrochemical profile of polysulfides in the electrolyte (1 M NaOH and 0.5 M Na_2S_2) was investigated using the cyclic voltammetry (CV) and linear sweep voltammograms (LSVs) test. The tests proceeded in a three-electrode cell, and more details are given in the supplemental information. As shown in Figures 1C and S2, the potential window of the SRR-SOR was located between the potential of the HER-OER at the same current density. The potential of SRR-SOR was only 0.15 V at a

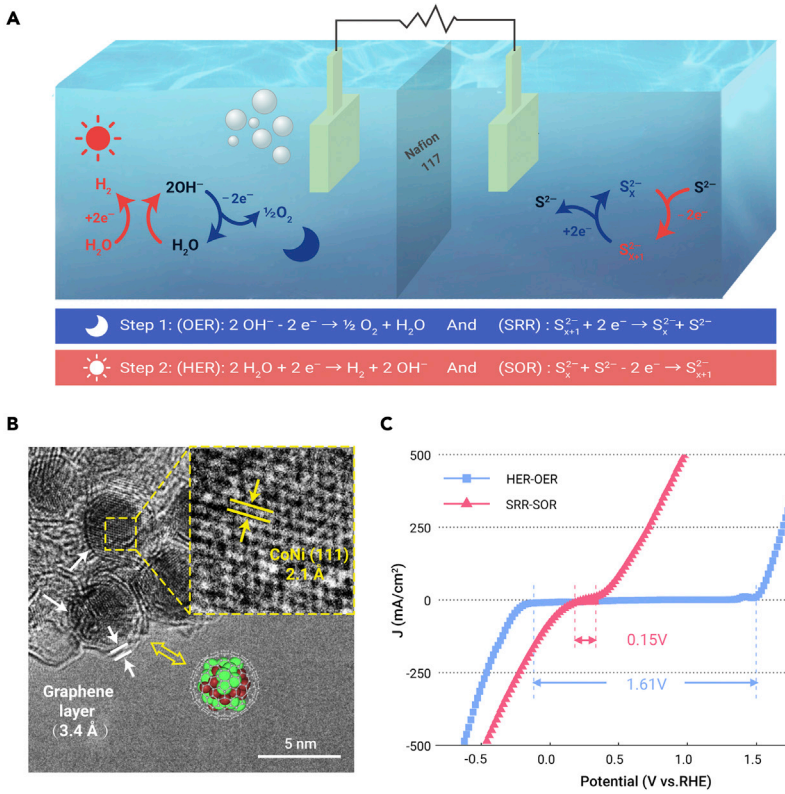

Figure 1. Decoupled device of water electrolysis (A) A schematic of the decoupled electrolyzer. Step 1 (O_2 production) involved the anodic OH^- oxidization for OER ($2OH^- - 2e^- \rightarrow ½O_2 + H_2O$) and the cathodic polysulfides reduction for SRR ($S_{x+1}^{2-} + 2e^- \rightarrow S_x^{2-} + S^{2-}$, x = 1–4). Step 2 ($H_2$ production) involved the cathodic H_2O reduction for HER ($2H_2O + 2e^- \rightarrow H_2 + 2OH^-$) and anodic polysulfides oxidation for SOR ($S_x^{2-} + S^{2-} - 2e^- \rightarrow S_{x+1}^{2-}$, x = 1–4).
(B) TEM image of CoNi@NGs. The insert schematic illustration shows the model structure of the CoNi@NGs. An enlargement of the dotted frame shows the (111) crystal plane of the CoNi alloy. The white marks show that the layer thickness of the single graphene layer was 3.4 Å.
(C) Comparison of SRR-SOR and HER-OER polarization curves of CoNi@NGs. At the current density of 10 mA/cm^2, the potential of HER-OER was 1.61 V and the SRR-SOR was 0.15 V. The experiments were carried out in a three-electrode cell, with 1 M NaOH and 0.5 M Na_2S_2 electrolyte at 25°C.

current density of 10 mA/cm^2. It was much lower than the potential of the HER-OER process, which needed 1.61 V. This result indicated that polysulfides could become the redox mediator to decouple the electrolysis of water, as shown in Figure 1A. In addition, the SRR and SOR activities of CoNi@NGs were compared with the precious metal materials, 40% Pt/C and IrO_2. As shown in Figure S3, the current density of CoNi@NGs was 2-fold higher than 40% Pt/C and 8-fold higher than IrO_2 at the same potential. The increasing of the sulfides' concentration was beneficial to improving electrocatalytic activity for CoNi@NGs (Figure S4). The value of double-layer capacitances (Cdl) further indicated that the excellent performance of CoNi@NGs was due to its higher electrochemical surface area (ECSA) and higher intrinsic catalytic activity (Figure S5). With the efficient catalysis of CoNi@NGs, the anodic potential of SOR was much lower than OER, which was beneficial to reduce the energy consumption of H_2 production.

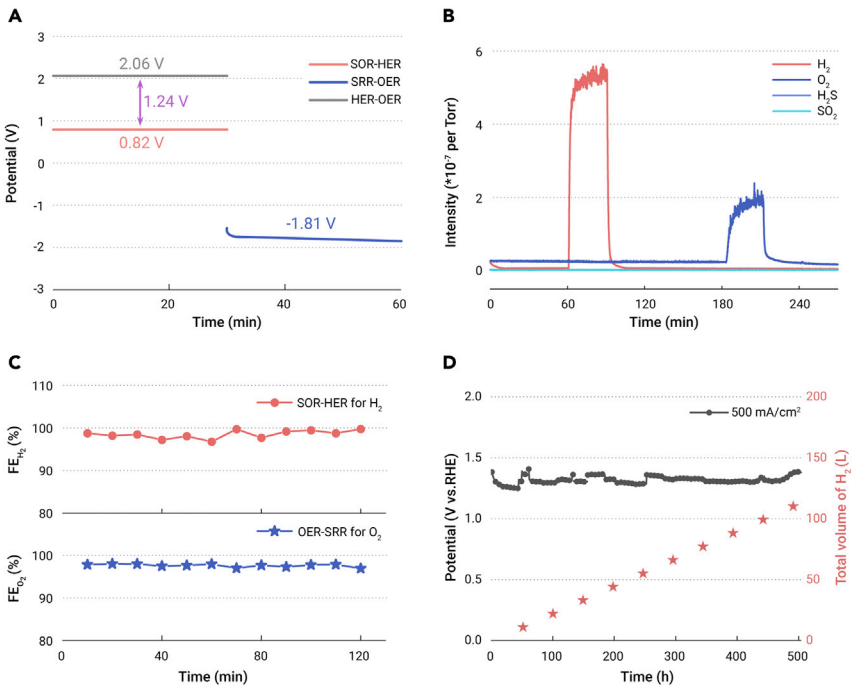

Figure 2. Performance of the decoupled electrolyzer (A) The comparison of the potential for decoupled water electrolysis with the one-step water electrolysis at a current density of 100 mA/cm^2.
(B) *In situ* electrochemical mass spectrometry curves of the H_2 evolution and O_2 evolution in the total decoupled water electrolysis process.
(C) *In situ* gas chromatography monitoring to test the Faradaic efficiency of H_2 and O_2 in a decoupled electrolysis process at a current density of 100 mA/cm^2.
(D) Capacity of maximum H_2 production in a single SOR-HER step. It produced H_2 in large quantities for 500 h with high current density of 500 mA/cm^2. The total volume of produced H_2 reached 112 L. All experiments were carried out in a three-electrode cell, with the 1 M NaOH and 1 M Na_2S electrolyte at 25°C.

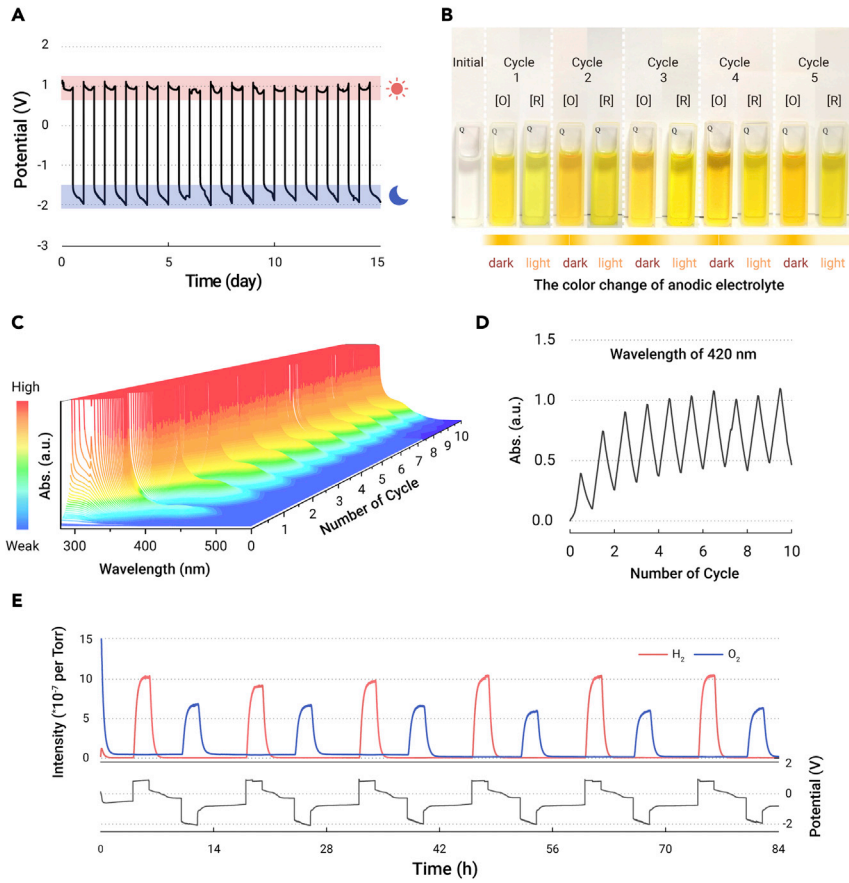

Figure 3. The cyclability of decoupled device (A) Cyclability test of the electrolyzer with a periodic alternation current density (100 mA/cm^2 in the daytime and −100 mA/cm^2 at night) for 15 cycles in 15 days.
(B–D) *In situ* UV-vis tests for the anodic electrolyte corresponding to successive process with 4 h per cycle (2 h SOR-HER and 2 h SRR-OER) for 10 cycles. The photograph in (B) corresponds to the electrolyte of the first five cycles in (C). The color depth of electrolyte changed alternately with the circulation of SOR ([O]) and SRR ([R]). The intensity of peak at 420 nm wavelength of (C) is shown in (D).
(E) *In situ* mass spectrometry curves of the H_2 evolution and O_2 evolution (up) corresponds to the total decoupled water electrolysis process (down) over six cycles. In one cycle, the reaction processed as follows: 4 h rest; 2 h SOR-HER step; 4 h rest; 2 h SRR-OER step; 2 h rest. All experiments were carried out in a two-electrode cell, with the 1 M NaOH and 0.5 M Na_2S_2 electrolyte at 25°C.

Performance of the decoupled electrolyzer

To realize the reaction process in Figure 1A, a decoupled electrolyzer was constructed and tested by the galvanostatic method in the three-electrode cell. As shown in Figure 2A, with a constant applied current density of 100 mA/cm^2, the potential of the SOR-HER step was only 0.82 V, and the following SRR-OER step proceeded at the potential of −1.81 V. The SRR-OER step of decoupled electrolysis could be driven by the surplus power at valley time, avoiding the electricity consumption in peak time. Therefore, the potential of the H_2 production step is only 0.82 V for proceeding SOR-HER. It decreased 1.24 V potential compared with one-step electrolysis of water, saving 60.2% of the electricity for H_2 production. It is the lowest potential of the H_2 evolution step compared with the reported decoupled electrolyzers at the same current density (Table S1). *In situ* electrochemical mass spectrometry was used to confirm the component of produced gas in the decoupled process. As shown in Figure 2B, only H_2 gas was produced in the SOR-HER step, and O_2 was the only gas product in the SRR-OER step. Thus, the gases produced in different steps were of high purity, which was convenient for collection and further utilization. By the real-time monitor of gas chromatography, it indicated that the Faradaic efficiency of H_2 and O_2 were both high, maintaining above 98% (Figure 2C). To further confirm H_2 production capacity in a single SOR-HER step, the electrolyzer was tested at a high current density of 500 mA/cm^2. As shown in Figure 2D, it kept producing H_2 for 500 h with a stable potential maintained around 1.2 V. The capacity of H_2 production reached 2.5 ×10^5 mAh/cm^2, and 112 L of H_2 was produced according to the measured Faradaic efficiency. It displayed the highest capacity for H_2 evolution in a single step of the previously reported decoupled devices (Table S1). The structures of CoNi@NGs were not damages after a 500-hour reaction, with metal cores being completely encapsulated in graphene shells (Figure S6). In the SRR-OER step, the electrolyzer also showed good durability in a 500-h reaction under the high-current-density test conditions (Figure S7). It further demonstrated that the electrolyzer had an excellent capacity for converting surplus electricity to hydrogen energy in large quantities. The above results indicate that this electrolyzer possessed high performance in the decoupled electrolysis of water, which efficiently achieved the production of voluminous H_2 with low energy consumption.

Cyclability of decoupled device in the circulation

To further confirm the cyclability of polysulfides, alternating galvanostatic tests have been performed in a two-electrode system. In order to simulate the peak regulation, the applied current density of ±100 mA/cm^2 (oxidized current was positive, and reduced current was negative) was periodically changed every 12 h with the alternation of day and night. The potential of electrolyzer maintained stability for 15 days in successive cycles (Figure 3A), around 0.9 V for the SOR-HER step and −1.8 V for the SRR-OER step. Ultraviolet-visible (UV-vis) spectrophotometry indicated that the concentration of polysulfides redox could return to the initial state after circulation (Figure S8). In order to observe the polysulfides redox in the electrolyte, an *in situ* electrochemical UV-vis spectrophotometry system was designed. In successive cycles, the color of electrolyte changed alternately, which became darker after SOR steps and light after SRR steps (Figure 3B). The corresponding *in situ* UV-vis results showed that the intensity of peaks at 300 nm and 420 nm changed periodically, which increased after the SOR step and decreased after the SRR step (Figures 3C, 3D, and S9). In addition, the evolution of gases was detected by the *in situ* mass spectrometry. As shown in Figure 3E, H_2 and O_2 were produced alternately as the potential changes. The produced gas was pure, without the mixture of H_2 and O_2 in respective steps. The above results demonstrate the polysulfides redox had excellent cyclability by the catalysis of CoNi@NGs, so that this decoupled device could run enduringly for a long time. Considering the advantages of simple and cheap synthesis, the polysulfides were proved to be a promising redox mediator in the decoupled electrolysis system.

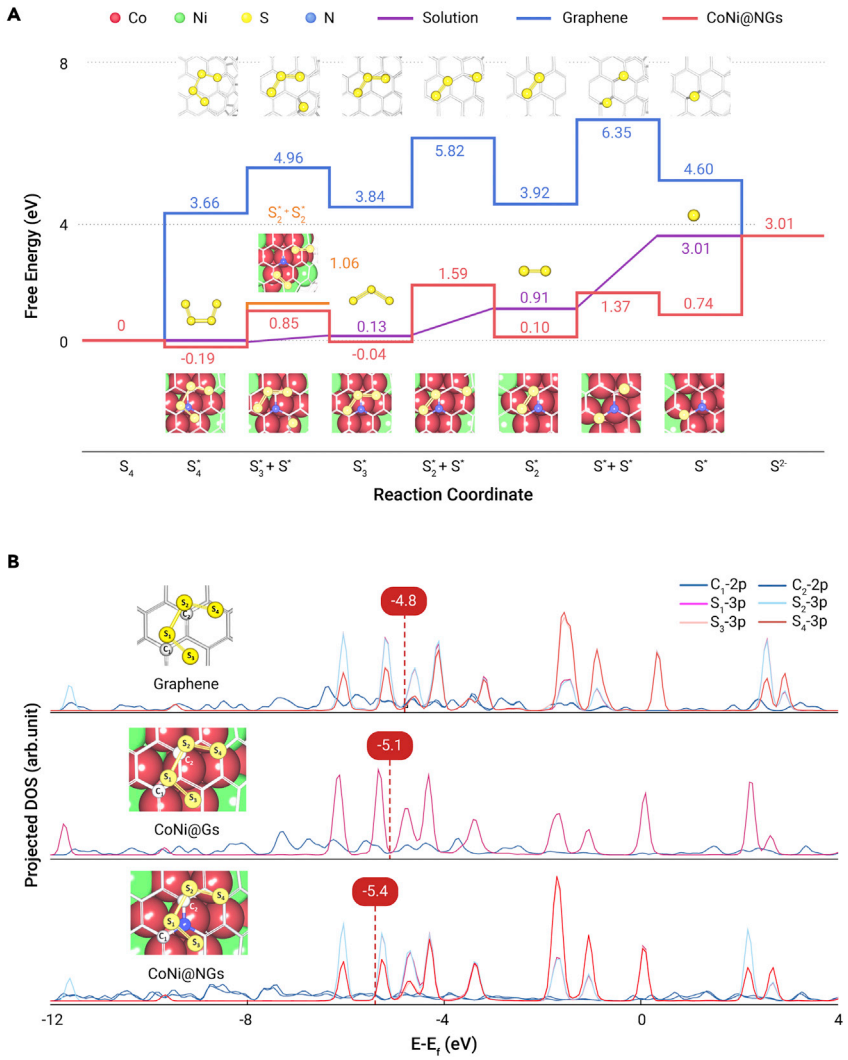

Figure 4. Theoretical interpretation of the SRR over CoNi@NGs (A) Free energy diagrams at −0.476 V for the SRR mechanism in the solution, on the graphene and CoNi@NGs surface based on DFT calculations. For each intermediate, a ball-and-stick model of the surface adsorbate configuration is shown. Gray, blue, red, green, yellow spheres represent C, N, Co, Ni, and S atoms respectively.
(B) Comparison of the projected DOS of S(3p) and its bonded C(2p) when S_4 was adsorbed on the surface of pristine graphene, CoNi@Gs, and CoNi@NGs. The dashed lines represent the centers of the occupied bands.

Mechanism calculation of polysulfides redox conversion

Density functional theory (DFT) calculations were performed to get more insight into the recycle of polysulfides redox on CoNi@NGs. As the mechanisms of SOR on the CoNi@NGs have been investigated, we here focus on the mechanism of SRR.[13] It is proposed that CoNi@NGs involves the adsorption of S_4 on the C site, which gets converted to S_4*, which gradually dissociates to S_3*, S_2*, S*, and finally results in the evolution of S^{2-} (Figure S10). The corresponding free energy profiles are given in Figure 4A. The results showed that the short-chain S_4*, S_3*, and S_2* species could be readily adsorbed on the carbon layer of CoNi@NGs and the adsorption free energies were near 0 eV. However, the processes of each dissociation step of adsorbed S_n* into co-adsorbed S_{n-1}*+S* were endothermic due to S–S bond breaking. The rate-determining step was the dissociation of S_3* to S_2*+S*. In addition to the investigation of S_3*+S* as the first dissociation product, the co-adsorbed species S_2*+S_2* originating from S_4* was also examined. The adsorption free energy of S_2*+S_2* was 0.21 eV higher than that of S_3*+S*, indicating that the splitting of S_4* to S_3*+S* may be preferred as the initial SRR dissociation step.

Following the formation of co-adsorbed S_n*+S*, the reduction step occurs with the adsorbed S* reduced into S^{2-} and removed from the surface, whereas the remaining S_n* stayed on the carbon ready for the following dissociation. The first reduction step of S_3*+S* was exothermic with a reaction energy of −0.89 eV. In the second reduction of S_2*+S* into S_2*, the reaction energy changed to significantly exothermic at −1.49 eV. For comparison, the free energy diagrams for SRR on the graphene surface, N-doped graphene, CoNi@Gs, and in the aqueous solution were also calculated (Figures 4A and S11). It was found that the free energies of the intermediates of each reaction step were lowest over CoNi@NGs among all studied catalysts. Furthermore, the calculated projected density of states (DOS) in Figure 4B showed that the band center of the occupied states of the C–S bond on CoNi@NGs located in a more negative energy regime, which means a stronger chemical bonding between S atom and C atom to enhance the S adsorption on the graphene surface. Thus, a superior SRR activity of CoNi@NGs catalyst would be expected from a thermodynamics viewpoint, which is consistent with the experimental observations.

CONCLUSIONS

In summary, we have successfully constructed a decoupled device by using polysulfides as redox mediators and CoNi@NGs as catalysts. By decoupling electrolysis of the water, we realized the conversion of surplus electricity to hydrogen energy. With the efficient catalysis of the CoNi@NGs, the potential of H_2 evolution was only 0.82 V at a current density of 100 mA/cm^2, which reduced 1.24 V compared with direct electrolysis of water. It displayed the excellent H_2 production capacity in quantity during one step, which reached 2.5×10^5 mAh/cm^2. Meanwhile, the polysulfides in the electrolyzer showed remarkable cyclability during the 15-day circulation tests without any decay. Further DFT calculations addressed the high recycle performance of polysulfides redox that originated from the electron transfer from the encapsulated metal alloy and N dopant to the graphene's surface. It modulated the

electronic structure of the graphene shell and facilitated the formation and decomposition of polysulfide intermediates. This work demonstrated that co-operating polysulfides redox with CoNi@NGs electrocatalyst could develop a kind of high-performance electrolyzer in the decoupled process of water electrolysis. It provides a new route to the rational use of electricity in a separate period, which is helpful to construct smart power grids for practical applications.

REFERENCES

1. Roberts, B.P., and Sandberg, C. (2011). The role of energy storage in development of smart grids. Proc. IEEE ***99***, 1139–1144. https://doi.org/10.1109/jproc.2011.2116752.
2. Jia, C., Pan, F., Zhu, Y.G., et al. (2015). High-energy density nonaqueous all redox flow lithium battery enabled with a polymeric membrane. Sci. Adv. ***1***. e150088626702440. https://doi.org/10.1126/sciadv.1500886.
3. Lubitz, W., and Tumas, W. (2007). Hydrogen: an overview. Chem. Rev. ***107***, 3900–3903. https://doi.org/10.1021/cr050200z.
4. Yang, D., Zhu, Q., and Han, B. (2020). Electroreduction of CO_2 in ionic liquid-based electrolytes. The Innovation ***1***. https://doi.org/10.1016/j.xinn.2020.100016.
5. Yuan, Y., Adimi, S., Thomas, T., et al. (2021). Co_3Mo_3N—an efficient multifunctional electrocatalyst multifunctional electrocatalyst. The Innovation ***2***. https://doi.org/10.1016/j.xinn.2021.100096.
6. Chen, L., Dong, X., Wang, Y., et al. (2016). Separating hydrogen and oxygen evolution in alkaline water electrolysis using nickel hydroxide. Nat. Commun. ***7***, 11714. https://doi.org/10.1038/ncomms11741.
7. Wallace, A.G., and Symes, M.D. (2018). Decoupling strategies in electrochemical water splitting and beyond. Joule ***2***, 1390–1395. https://doi.org/10.1016/j.joule.2018.06.011.
8. Amstutz, V., Toghill, K.E., Powlesland, F., et al. (2014). Renewable hydrogen generation from a dual-circuit redox flow battery. Energy Environ. Sci ***7***, 2350–2358. https://doi.org/10.1039/c4ee00098f.
9. Symes, M.D., and Cronin, L. (2013). Decoupling hydrogen and oxygen evolution during electrolytic water splitting using an electron-coupled-proton buffer. Nat. Chem. ***5***, 403–409. https://doi.org/10.1038/nchem.1621.
10. Ma, Y., Guo, Z., Dong, X., et al. (2019). Organic proton-buffer electrode to separate hydrogen and oxygen evolution in acid water electrolysis. Angew. Chem. Int. Ed. ***58***, 4622–4626. https://doi.org/10.1002/anie.201814625.
11. Landman, A., Halabi, R., Dias, P., et al. (2020). Decoupled photoelectrochemical water splitting system for centralized hydrogen production. Joule ***4***, 448–471. https://doi.org/10.1016/j.joule.2019.12.006.
12. Lim, J., Pyun, J., and Char, K. (2015). Recent approaches for the direct use of elemental sulfur in the synthesis and processing of advanced materials. Angew. Chem. Int. Ed. ***54***, 3245–3249. https://doi.org/10.1002/anie.201409468.
13. Zhang, M., Guan, J., Tu, Y., Chen, S., et al. (2020). Highly efficient H_2 production from H_2S via a robust graphene-encapsulated metal catalyst. Energy Environ. Sci. ***13***, 119–126. https://doi.org/10.1039/C9EE03231B.

ACKNOWLEDGMENTS

We gratefully acknowledge the financial support from the Ministry of Science and Technology of the People's Republic of China (no. 2016YFA0204100 and 2016YFA0200200), the National Natural Science Foundation of China (no. 21890753 and 21988101), the Key Research Program of Frontier Sciences of the Chinese Academy of Sciences (no. QYZDB–SSW–JSC020), the DNL Cooperation Fund, CAS (no. DNL180201), the Natural Science Foundation of Shandong Province (ZR2019MEE015), and the Key Research and Development Plan of Shandong Province (2018GSF117042).

AUTHOR CONTRIBUTIONS

D.D. conceived the project and designed the experiments. M.Z., Y.T., and S.W. performed the materials synthesis, characterization, and electrochemical measurements. J.G. conducted the DFT calculations. M.Z., J.G., and D.D. co-wrote the manuscript.

DECLARATION OF INTERESTS

The authors declare no competing interests.

LEAD CONTACT WEBSITES

http://deng.dicp.ac.cn.

SUPPLEMENTAL INFORMATION

Supplemental information can be found online at https://doi.org/10.1016/j.xinn.2021.100144.